0026-895X/00/050948-06$3.00/0
MOLECULAR PHARMACOLOGY

MOL 57:948–953, 2000 /13003/817848

The Mechanism of Phosphorylation of Anti-HIV D4T by Nucleoside Diphosphate Kinase[1]

BENOIT SCHNEIDER, RICARDO BIONDI,[2] ROBERT SARFATI, FABRICE AGOU, CATHERINE GUERREIRO, DOMINIQUE DEVILLE-BONNE, and MICHEL VERON

Unité de Régulation Enzymatique des Activités Cellulaires, Centre National de la Recherche Scientifique, Unité de Recherche Associée 1773 (B.S., R.B., F.A., D.D-B., M.V.), and Unité de Chimie Organique, Centre National de la Recherche Scientifique, Unité de Recherche Associée 2128, 558 (R.S., C.G.), Institut Pasteur, Paris, France

Received September 29, 1999; accepted January 20, 2000

This paper is available online at http://www.molpharm.org

ABSTRACT

The last step in the intracellular activation of antiviral nucleoside analogs is the addition of the third phosphate by nucleoside diphosphate (NDP) kinase resulting in the synthesis of the viral reverse transcriptase substrates. We have previously shown that dideoxynucleotide analogs and 3′-deoxy-3′-azidothymidine (AZT) as di- or triphosphate are poor substrates for NDP kinase. By use of protein fluorescence, we monitor the phosphotransfer between the enzyme and the nucleotide analog. Here, we have studied the reactivity of D4T (2′,3′-dideoxy-2′,3′-didehydrothymidine; stavudine) as di- (DP) or triphosphate (TP) at the pre-steady state. The catalytic efficiency of D4T-DP or -TP is increased by a factor of 10 compared with AZT-DP or -TP, respectively. We use an inactive mutant of NDP kinase to monitor the binding of a TP derivative, and show that the affinity for D4T-TP is in the same range as for the natural substrate deoxythymidine triphosphate, but is 30 times higher than for AZT-TP. Our results indicate that D4T should be efficiently phosphorylated after intracellular maturation of a prodrug into D4T-monophosphate.

Nucleoside analogs AZT and D4T are powerful anti-HIV drugs that are now generally used in combination with 3TC (β-L-2′,3′-dideoxy-3′-thiocytidine) and either an antiprotease or a non-nucleosidic reverse transcriptase inhibitor in tritherapy protocols (Foudraine et al., 1998). The pharmacological target of AZT and D4T is the HIV reverse transcriptase because both analogs act as DNA chain terminators due to the lack of 3′-OH in their ribose moiety. However, to exert their antiviral activity, the nucleoside analogs must be activated into triphosphate derivatives by cellular kinases. Intracellular accumulation of mono or diphospho compounds due to kinetically limiting steps in this phosphorylation pathway could be responsible for some of the toxic effects of the drugs, in particular at the mitochondrial level (Zhu et al., 1998). The last step in this pathway is catalyzed by NDP kinase. Although this enzyme is generally not specific for the base and accepts deoxyribonucleotides, we showed that the phosphorylation of AZT-DP and ddNDP by NDP kinase is very slow and could constitute a limiting step in the overall phosphorylation pathway (Bourdais et al., 1996; Schneider et al., 1998b).

NDP kinase catalyzes the phosphotransfer from NTP to NDP with the transient phosphorylation of a histidine at the active site (Garces and Cleland, 1969). The X-ray structures of NDP kinases from several species have been determined at high resolution (Williams et al., 1991; Dumas et al., 1992; Chiadmi et al., 1993; Webb et al., 1995), showing that both the subunit fold and structure of the active site are highly conserved. The mode of nucleotide binding to the protein is different from that of most kinases because the base makes no polar interactions with the protein and is at the protein surface. The ribose and phosphate moieties are located deeper inside the NDP kinase active site, forming numerous bonds with a Mg^{2+} ion and with protein side chains. The enzyme-nucleotide complex is also stabilized by a hydrogen bond network between the 3′-OH of the sugar, the β-phos-

[1] This work was supported by funds from Agence Nationale de la Recherche contre le SIDA, the Association de la Recherche sur le Cancer, and from SIDACTION. R. B. was recipient of a fellowship from Fondation de la Recherche Médicale. This work has been presented as a poster presentation at Gordon Research Conferences, Purines, pyrimidines and related substances, Salve Regina University, University of Rhode Island, Kingston, RI, July 4–9,1999, and at the 7th Symposium of the European Society for the Study of Purine & Pyrimidine Metabolism in Man, Gdansk, Poland, September 15–19, 1999.

[2] Present address: Division of Signal Transduction Therapy, University of Dundee, UK.

ABBREVIATIONS: AZT, 3′-deoxy-3′-azidothymidine; DP, diphosphate; MP, monophosphate; TP, triphosphate; Dd-NDPK, *Dictyostelium* nucleoside diphosphate kinase; D4T, 2′,3′-didehydro-2′,3′-dideoxythymidine; ddTTP, 2′,3′-dideoxythymidine triphosphate; ddNDP, 2′,3′-dideoxynucleotide diphosphate; ddNTP, 2′,3′-dideoxynucleotide triphosphate; NDP, nucleoside diphosphate; NDPK-A, human nucleoside diphosphate kinase type A; NTP, nucleoside triphosphate; PMSF, phenylmethylsulfonyl fluoride, TK, thymidine kinase; DTE, dithioerythritol.

phate, and two conserved residues of the active site, Lys16 and Asn119 (Tepper et al., 1994).

All eukaryotic NDP kinases are hexamers made of identical 17-kDa monomers. In humans, in whom five isoforms have been reported, the major forms are NDPK-A and NDPK-B, which are encoded, respectively, by the genes *nm23-H1* and *nm23-H2* and display 88% amino acid identity. The other members of the family include DR-*nm23,* involved in apoptosis (Venturelli et al., 1995), the mitochondrial *nm23*-H4 (Milon et al., 1997), and *nm23*-H5, found in testis germ cells but devoid of enzymatic activity (Munier et al., 1998). Human A and B enzymes present similar kinetic parameters for natural substrates (Schaertl et al., 1998) as well as for a series of thymidine diphosphate derivatives (Gonin et al., 1999). Both the structure and the kinetic parameters of the NDP kinase from the lower eukaryote *Dictyostelium discoideum* (Dd-NDPK) are also very similar to those of human NDPK-A or NDPK-B, and this has allowed us to use Dd-NDPK as a reliable model for eukaryotic NDP kinases. The structure of Dd-NDPK was also solved in the presence of ADP and AlF_3 which led to modeling of the transition state and the catalytic mechanism (Xu et al., 1997a).

NDP kinase has a very high turnover with k_{cat} around 1000 s^{-1} for "natural" ribo- or deoxyribonucleotides. The fluorescence properties of NDP kinases allowed us to monitor the degree of phosphorylation of the catalytic histidine (Deville-Bonne et al., 1996), and we have shown by steady-state enzymatic assays that AZT-TP and ddTTP are poor substrates for NDP kinase, with a loss in catalytic efficiency in the 10^4 to 10^5 range as compared with natural nucleotides (Bourdais et al., 1996). Using stopped-flow experiments, we showed that this loss is due to a dramatic decrease in the phosphate transfer rate between the analog and the enzyme (Schneider et al., 1998b).

AZT and D4T are both thymidine analogs and are presumably phosphorylated by the same cellular kinases. However, their patterns of intracellular phosphorylation are not the same because, in particular, D4T is phosphorylated to its 5′-monophosphate at a level 500-fold lower than AZT is (Balzarini et al., 1989; Gao et al., 1994). In this work we have used pre-steady-state and steady-state experiments to investigate kinetic parameters of human NDPK-A with D4T-DP or D4T-TP as a substrate. We show that D4T-DP is more easily phosphorylated by NDPK-A than is AZT-DP. The use of an inactive mutant of Dd-NDPK allowed us to investigate for the first time the binding of NTPs to NDP kinase in the absence of catalysis. We show that D4T-TP binds to the NDP kinase active site with an affinity similar to that of natural substrates, whereas AZT-TP is a weaker ligand.

Experimental Procedures

Materials. Natural nucleotides were from Roche Molecular Biochemicals. The chemical synthesis of phosphoderivatives of nucleoside analogs was as described previously (Bourdais et al., 1996). The double mutation F64W-H122G in Dd-NDPK was made by site-directed mutagenesis according to the method of Kunkel (1985), with the oligonucleotides 5′-GAAAGACCAT**GG**TTCGGTGGTT-3′ and 5′-GAAACATCATC**GG**CGGTTCTGATTC-3′ for the F64W and H122G mutations, respectively. Altered bases as compared with the wild-type sequence are bold underlined. The mutations were verified by DNA sequencing.

Enzyme Purification. Wild-type human NDPK-A was overexpressed in *Escherichia coli* (BL21-DE3) by using plasmid pJC20 (gift from M. Konrad) after induction for 5 h by 1 mM isopropylthiogalactoside when the culture reached $A_{600\ nm} \approx 0.5$. Cells were collected, washed twice, and resuspended in extraction buffer (50 mM Tris-HCl, pH 8.0, 20 mM KCl, 1 mM EDTA, 5 mM $MgCl_2$, and 1 mM DTE) containing 1 mM phenylmethylsulfonyl fluoride. The cell extract was diluted 2.5-fold with extraction buffer and centrifuged at 10,000*g* for 20 min at 4°C. The supernatant was treated by 0.15% Polymin *P* (BASF) to precipitate most of the nucleic acids. After centrifugation at 10,000*g* for 15 min, the supernatant was loaded at pH 8.0 onto a POROS HQ column (PerSeptive Biosystems, Cambridge, MA; 2.6 × 12 cm) equilibrated in 50 mM Tris-HCl, pH 8.0, 1 mM EDTA, and 1 mM DTE. The recombinant enzyme was separated from the *E. coli* NDP kinase by a linear KCl gradient (0.02–1 M). Active fractions measured as in Lascu et al. (1992) were pooled, diluted 2-fold with 100 mM Bis-Tris, pH 6.0 and DTE 1 mM, and loaded onto a ceramic hydroxyapatite column (American International Chemical, 1.6 × 10 cm) equilibrated in 10 mM potassium phosphate, pH 6.5, and 1 mM DTE. NDPK-A was eluted by a linear potassium phosphate gradient (0.01–1 M). After concentration and desalting by ultrafiltration in 50 mM Tris-HCl, pH 7.5, 1 mM DTE, and 20 mM KCl, the enzyme was extensively dialyzed against the same buffer containing 50% glycerol and stored at −20°C. NDPK-A was > 97% pure as judged by SDS-PAGE. Wild-type and mutant Dd-NDPK were overexpressed in *E. coli* (XL1-Blue) and purified as previously described (Schneider et al., 1998a). Enzyme concentration expressed as 17-kDa subunits was determined either by the method of Bradford (1976) or by using an absorbance coefficient of $\Delta A_{280} = 1.238$, 0.55, and 0.85 for a 1 mg/mL solution of NDPK-A, Dd-NDPK, and the double mutant F64W-H122G, respectively (Gill and Von Hippel, 1989). F64W-H122G mutant NDP kinase had no measurable NDP kinase activity but had a very slight ATPase activity ($k_{cat}/K_M = 450\ M^{-1}\ s^{-1}$).

Fluorometric Binding Studies. The affinity of NDP and NTP derivatives for NDP kinase was determined by following the variation of the intrinsic fluorescence upon nucleotide binding as described in Schneider et al. (1998b). The fluorescence of the F64W-H122G enzyme in T_1 buffer (50 mM Tris-HCl, 75 mM KCl, 5 mM $MgCl_2$, pH 7.5) was measured at 330 nm with excitation at 310 nm (2-nm excitation slit and 4-nm emission slit). Successive aliquots of nucleotide were added to a 1 μM enzyme solution. The inner filter effect was negligible. Experimental binding curves were fitted to a quadratic equation for ligand-protein curve after correction for dilution. By using the double mutant with NTP, the true NTP concentration was measured in order to take into account the small residual ATPase activity. The correction was less than 2%.

Stopped-Flow Kinetic Experiments. Stopped-flow kinetic experiments were performed with a Hi-Tech DX2 microvolume stopped-flow reaction analyzer equipped with a high intensity xenon lamp as described (Schneider et al., 1998b). The excitation wavelength was 304 nm, with a 2-mm excitation slit and a 320-nm cutoff filter at the emission. Mixing was achieved in less than 2 ms. After mixing NDPK (1 μM) and NTP (10–500 μM) or phosphorylated NDPK and NDP, the intrinsic protein fluorescence was recorded for 10 to 200 s. In each experiment 400 pairs of data were recorded, and the data from three to four identical experiments were averaged and fitted to a number of nonlinear analytical equations using the software provided by Hi-Tech. All curves fitted to single exponentials.

Analysis of Kinetic Results. As previously described (Schneider et al., 1998b), the data were analyzed with the reaction scheme:

$$E + NTP \underset{k_{-1}}{\overset{k_{+1}}{\leftrightarrow}} E \cdot NTP \underset{k_{-2}}{\overset{k_{+2}}{\leftrightarrow}} E \sim P{\cdot}NDP \underset{k_{-3}}{\overset{k_{+3}}{\leftrightarrow}} E \sim P + NDP \qquad (1)$$

(Reaction 1)

The observed single step could be attributed to the phosphotransfer between the nucleotide and the enzyme in both directions. In both the forward and the reverse reactions, the product concentration

remains very low; thus, the product binding can be neglected. The binding steps are expected to be fast in both directions and are not detectable in the time range of the stopped-flow experiments. Saturation could not be obtained with the concentrations of AZT-TP and D4T-TP used here. Therefore, we measured the catalytic efficiency of the enzyme phosphorylation (CE_{phos}) and the catalytic efficiency of phosphoenzyme dephosphorylation (CE_{dephos}), which are equivalent to second order constants and allow a reliable comparison of a variety of NDP kinase substrates.

Results

Kinetics of D4T Phosphorylation and Dephosphorylation by NDP Kinase. The intrinsic fluorescence of NDP kinase decreases upon phosphorylation of the catalytic histidine, providing a convenient signal for probing the state of phosphorylation of the enzyme (Schneider et al., 1998b). Figure 1A shows the time course of this fluorescence decrease when human NDPK-A is mixed rapidly with different phos-

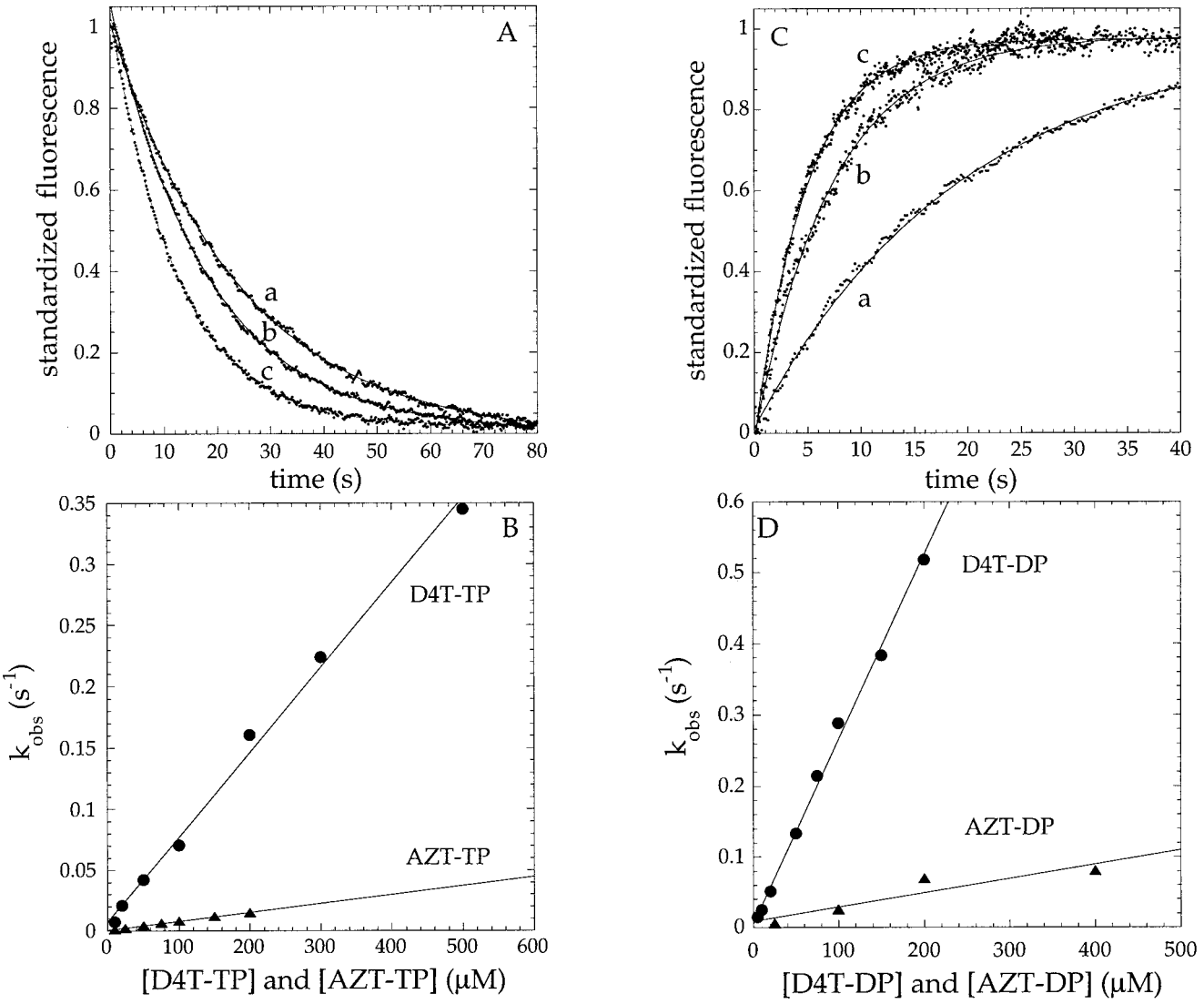

Fig. 1. Pre-steady-state kinetics of phosphotransfer between NTP analogs and NDPK (A and B) and between the phosphorylated NDPK and NDP analogs (C and D). A, kinetics of phosphorylation of NDPK-A by D4T-TP. The enzyme (1 μM, final concentration) in T_2 buffer (50 mM Tris-HCl, pH 7.5, 5 mM $MgCl_2$, 75 mM KCl, 1 mM DTE, and 5% glycerol) at 20°C was rapidly mixed with D4T-TP (50, 100, and 200 μM, respectively, for curves a, b, and c). The decrease in fluorescence was monitored with time on the stopped-flow device (λ_{exc} = 304 nm, emission filter < 320 nm). Each reaction was monitored during 200 s. The data were plotted on the scale 0 to 80 s for clarity. The solid lines represent the best fit of each curve to a monoexponential. B, concentration dependence of the phosphorylation rate constant upon D4T-TP or AZT-TP concentration. The pseudo-first order rate constant for the reaction (k_{obs}) was plotted against analog triphosphate: D4T-TP (●) and AZT-TP (▲). The linear fit indicates that data can be analyzed as a second order reaction (see *Experimental Procedures*). The apparent second order rate constant is 700 M^{-1} s^{-1} for D4T-TP and 75 M^{-1} s^{-1} for AZT-TP. C, kinetics of dephosphorylation of phosphorylated NDPK-A by D4T-DP. Phosphorylated enzyme was prepared and the stoichiometry of phosphorylation was determined as described (Deville-Bonne et al., 1996) with small modifications for human NDPK. NDPK-A was preincubated with a saturating amount of ATP in T_2 buffer. The phosphorylated enzyme (1 μM, final concentration) in T_2 buffer at 20°C was rapidly mixed with D4T-DP (40, 100, and 150 μM, respectively for curves a, b, and c). The increase in fluorescence was monitored with time on the stopped-flow device. The solid lines represent the best fit of each curve to a monoexponential. D, concentration dependence of the phosphotransfer rate constant on D4T-DP or AZT-DP concentration. The pseudo-first order rate constant for the reaction (k_{obs}) was plotted against analog diphosphate: D4T-DP (●) and AZT-DP (▲). The linear fit indicates that data can be analyzed as a second order reaction with an apparent constant of 2600 M^{-1} s^{-1} for D4T-DP and 200 M^{-1} s^{-1} for AZT-DP.

phodonors. Addition of D4T-TP results in an exponential decrease in fluorescence leading to a plateau which corresponds to the steady-state of the phosphorylation reaction. Each recorded fluorescence time course follows a single decay with no evidence of lag, burst, or biphasicity. Whereas the amplitude of the fluorescence change is almost constant, the constant of the exponential representing the rate constant of the phosphorylation reaction is linear with the concentration of the phosphodonor in the range 10 to 500 μM (Fig. 1B).

With the concentrations of AZT and D4T derivatives used in this study, saturation could not be obtained due to the small amounts of compound available. Therefore, the only parameter that can be attributed with confidence are the constants CE_{phos} and CE_{dephos} characterizing the phosphorylation and the dephosphorylation reactions, respectively. Table 1 lists the values of these constants corresponding to the slope of the representations in Fig. 1, B and D, for several analogs. The phosphorylation of NDPK-A by D4T-TP (CE_{phos}, = 700 M^{-1} s^{-1}) is 10 times faster than by AZT-TP (CE_{phos} = 75 M^{-1} s^{-1}) and 30 times faster when compared with ddTTP (CE_{phos} = 20 M^{-1} s^{-1}). Note that, even for D4T, the values of CE_{phos} are low compared with natural nucleotides. Table 1 also shows that similar results are obtained with Dd-NDPK, indicating that this protein can serve as a model for the study of analog phosphorylation. ddTTP is, however, a slightly better substrate than AZT-TP, as previously shown (Schneider et al., 1998b).

The rate of dephosphorylation of phosphorylated NDPK-A in the presence of D4T-DP and other diphospho-derivatives also displays a monoexponential time course (Fig. 1C). For D4T-DP the rate constants of dephosphorylation are about 5 times higher than for phosphorylation at the same nucleotide concentration, in agreement with Haldane relationships (Garces and Cleland, 1969; Schneider et al., 1998b). The slope of the variation of this rate constant as a function of nucleotide analog concentration (Fig. 1D) represents the catalytic efficiency for dephosphorylation (CE_{dephos}). As shown in Table 1, CE_{dephos} is 12 times greater for D4T-DP than for AZT-DP.

The kinetic parameters of the steady-state reaction were also measured with use of a coupled assay (Lascu et al., 1992). The catalytic efficiencies of the enzyme (Table 2) are in excellent agreement with the values found in pre-steady-state experiments, indicating that the phosphotransfer step between the phosphorylated NDPK-A and D4T-DP is the limiting step of the enzymatic reaction in excess of ATP. The increased activity of NDPK-A with D4T derivatives as compared with AZT could result from a better binding affinity of D4T-TP to the active site or to a specific ability of D4T to orient the phospho-accepting group toward the catalytic histidine. Several experiments were designed to distinguish between these possibilities.

Measure of the Affinity of NDP Kinase for NTP. Up to now, all previous affinity measurements of nucleotides for NDPK have been made with NDP, as well as AZT-DP and ddNDP (Schneider et al., 1998b), because for NTP the γ-phosphate hydrolysis is too fast. However diphospho-compounds lead to the formation of "dead-end" complexes that are not normally part of the reaction, and it would be important to determine the true affinities of NDPK for its NTP substrates. To adress this question, we combined two previously characterized single mutations in the Dd-NDPK. The H122G mutation results in an inactive protein because it is unable to autophosphorylate. Crystal structure of the complex between the H122G enzyme and ADP. . . Pi-Mg^{2+} shows that the mutation does not affect the overall structure of the catalytic site (Admiraal et al., 1999). In contrast, the single mutant F64W, where the Phe 64 at the entrance of the active site is substituted to a Trp residue, is fully active. Moreover this Trp constitutes a fluorescent probe that is sensitive to NDP nucleobase stacking (Schneider et al., 1998b). Figure 2 (inset) shows the intrinsic fluorescence of F64W-H122G mutant NDP kinase. Upon excitation at 310 nm, the fluorescence intensity of the mutant protein increases by 50% upon any NTP and NDP addition.

The dissociation constants (K_D) for diphospho- and triphospho-derivatives were estimated from binding curves similar to that shown in Fig. 2. As shown in Table 3, the K_D values of NDP kinase for NTP are 100 times lower than for NDP, corresponding to a higher binding energy equivalent to 2.6 kcal/mol. Note that the relative affinities for the various NTPs are listed in the same order as their reported catalytic efficiency (Schaertl et al., 1998) or those measured with ddNTP derivatives (Schneider et al., 1998b). Moreover, the K_D values for the nonhydrolysable ATP analogs, AMP-PCP and AMP-PNP as well as for NDP, are similar whether measured with F64W or with F64W-H122G mutant NDP kinase. These results indicate that the absence of His122 side chain does not strikingly modify the affinity of a nucleotide for the active site, and that the values shown in Table 3 are similar to the true K_D of NTP for wild-type NDPK. However, the absence of H122 may relieve constraints and lead to some overestimation of the K_D for NTP. Note that AMP-PNP binds to the active site with higher affinity than does AMP-PCP due to the electronegative N: it is a donor in the intranucleotide H-bond with the hydroxyl in the 3′ position that is characteristic of a NDP kinase-bound nucleotide.

Table 3 also shows the affinity of D4T-TP (K_D = 1.2 μM), AZT-TP (K_D = 30 μM), and ddTTP (K_D = 4 μM) for the F64W-H122G mutant protein. Surprisingly, D4T-TP binds to

TABLE 1

Presteady state reaction of NDPK with thymidine analogs

Stopped-flow parameter values correspond to data from Fig. 1. All the experiments were performed at 20°C. Data correspond to three independent measurements. S.E. (not shown) amount to < 10%.

Phosphotransfer from XTP to E			Phosphotransfer from E~P to XDP		
XTP	Dd-NDPK	NDPK-A	XDP	Dd-NDPK	NDPK-A
	CE_{phos} (M^{-1} s^{-1})			CE_{dephos} (M^{-1} s^{-1})	
dTTP	5.7×10^6	1×10^6	dTDP	15×10^6	2×10^6
D4T-TP	11,500	700	D4T-DP	66,000	2,600
AZT-TP	270	75	AZT-DP	1,500	200
ddTTP	500	20	ddTDP		

the enzyme with a K_D similar to that of its natural counterpart dTTP (K_D = 1.2 μM). Thus, although no 3′-OH is present on the ribose moiety, D4T binds very efficiently to the enzyme. The binding of [^{14}C]ATP to the double mutant F64W-H122G NDP kinase was also determined by Hummel-Dreyer chromatography (Hummel and Dreyer, 1962). The K_D from this experiment gave a value in the micromolar range in excellent agreement with the fluorometric titrations described above (data not shown).

Discussion

In this paper, we show that the DP and the TP forms of D4T are considerably better substrates for NDP kinase than are AZT derivatives. D4T-TP also has a high affinity toward HIV reverse transcriptase and human DNA polymerase γ (Ono et al., 1989), possibly due to the planarity of the glycone cycle resulting in a unique conformation of the nucleotide, which allows the formation of a reaction complex with DNA polymerase and participates in the formation of the transition state (Krayevsky and Watanabe, 1998). In contrast, the presence of an azido group on the sugar moiety may restrict its mobility and prevent a planar conformation from occurring within the catalytic cycle. In agreement with this hypothesis, the deoxyribose is found C2′-endo in AZT-DP (Xu et al., 1997b), whereas it is C3′-endo for natural NDP (Cherfils et al., 1994; Morera et al., 1994, 1995). A precise structural explanation for the different efficiencies of AZT and D4T derivatives as substrates for NDP kinase is presently not available. However, we hypothesize a role of the conserved Lys (K16 in Dd-NDPK, K12 in NDPK-A) that participates in catalysis (Tepper et al., 1994). Indeed, the side chain of this lysine moves by more than 2.6Å upon binding of the bulky azido group (Xu et al., 1997b), and this probably results in the poor phosphorylation of AZT-DP by NDP kinases. The absence of steric hindrance in the D4T analog may leave the lysine in place, resulting in a better phosphorylation efficiency.

The three enzymes involved in the cellular phosphorylation pathway of thymidine derivatives, i.e., TK, thymidylate kinase, and NDP kinase, have very different efficiencies toward D4T and AZT (Balzarini et al., 1989). Whereas the critical steps in the AZT phosphorylation pathway are the reactions catalyzed by thymidylate kinase (Lavie et al., 1997) and NDP kinase (Schneider et al., 1998b), the pharmacological activation of D4T is mostly dependent upon its phosphorylation in D4T-MP (Balzarini et al., 1989). In vitro studies also show that D4T is a poor substrate for purified human TK1 and TK2 (Munch-Petersen et al., 1991). By using recombinant enzymes, we showed that, although D4T is a poor substrate for TK from *E. coli*, D4T-MP is a good substrate for *E. coli* thymidylate kinase (not shown). We show here that the phosphorylation of D4T-DP by NDP kinase is 10 times more efficient than that by AZT or ddNDPs. Our results highlight the potential interest for designing a prodrug to deliver D4T-MP inside cells to bypass the TK-dependent reaction step (Balzarini et al., 1996; Egron et al., 1998). Because D4T is already known to present less toxicity (Kaul

TABLE 2

Enzymatic study of NDPK activity at the steady state

Phosphorylation of dTDP analogs by ATP was measured. Steady-state parameter values of NDPK reaction are given with ATP as donor of phosphate and dTDP analogs as acceptor. All the experiments were performed at 20°C. Data correspond to three independent measurements. S.E. (not shown) amount to less than 10%.

XDP	Dd-NDPK	NDPK-A
	k_{cat}/K_m (M^{-1} s^{-1})	
dTDP	17×10^6	3×10^6
D4T-DP	65,000	2,650
AZT-DP	1,000	192

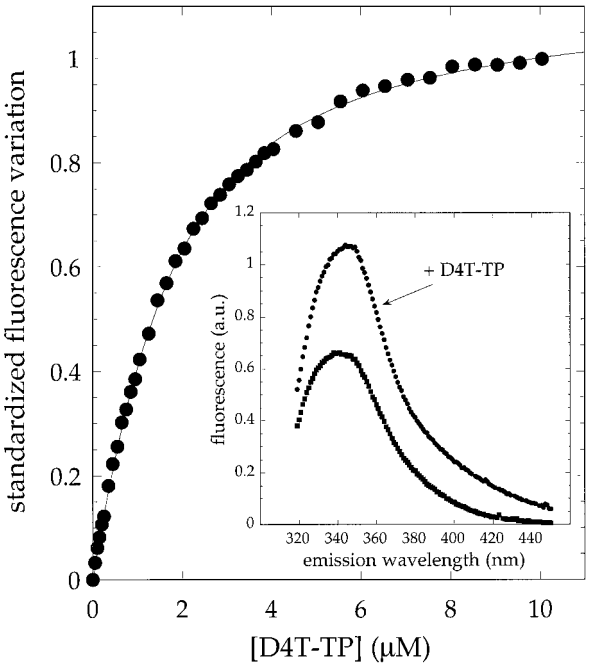

Fig. 2. Binding curve of F64W-H122G NDP kinase with D4T-TP. Fluorescence change of F64W-H122G NDPK (1 μM) upon binding of D4T-TP (●) at 20°C in buffer T_1, pH 7.5 (λ_{exc} = 310 nm, λ_{em} = 330 nm). The solid line is the best fit of the data to a quadratic saturation curve. It corresponds to a K_D of 1.2 ± 0.1 μM for D4T-TP (see also Table 3). Inset: fluorescence emission spectra of F64W-H122G NDPK (1 μM) in the absence and in the presence (dotted line) of 0.5 mM D4T-TP.

TABLE 3

Dissociation constants of F64W-H122G and F64W mutant NDPKs for NDPs, NTPs, and nonhydrolyzable ATP analogs

Titrations of F64W-H122G NDPK with natural and anti-HIV nucleotides were performed as described in the legend to Figure 2. Data presented are the mean values of three determinations ± S.E.

Nucleotide	F64W-H122G	F64W
	K_D (μM)	
dTTP	1.2 ± 0.1	n.m.
ddTTP	4.0 ± 0.6	n.m.
AZT-TP	30 ± 3	n.m.
D4T-TP	1.2 ± 0.1	n.m.
ATP	0.20 ± 0.05	n.m.
GTP	0.15 ± 0.05	n.m.
CTP	7.0 ± 1.0	n.m.
AMP-PNP	30 ± 3	60 ± 6
AMP-PCP	750 ± 100	1000 ± 200
dTDP	75 ± 20	100 ± 50[a]
AZT-DP	125 ± 10	80 ± 20[a]
D4T-DP	85 ± 10	no signal
ADP	25 ± 1	25 ± 5[a]
GDP	15 ± 2	14 ± 5[a]
CDP	210 ± 20	200 ± 100[a]

n.m., nonmeasurable.
[a] The binding of NDPs to F64W is measured as shown in Schneider et al. (1998b).

et al., 1999) and to elicit less resistance than AZT at the reverse transcriptase level, a prodrug of D4T should be efficiently phosphorylated after intracellular maturation into D4T-MP.

Acknowledgments

We thank Manuel Babolat for excellent technical assistance in purifications and stopped-flow experiments and Céline Costa for help in titrations. We also thank Manfred Konrad (Max Planck Institute, Göttingen, Germany) for the gift of plasmid, Ioan Lascu (Université Bordeaux II, France) for making results available before publication, and Joel Janin (LEBS, Gif sur Yvette, France) and Jeff Stock (Princeton University, Princeton, NJ) for stimulating discussions.

References

Admiraal SJ, Schneider B, Meyer P, Janin J, Véron M, Deville-Bonne D and Herschlag D (1999) Nucleophilic activation by positioning in phosphoryl transfer catalyzed by Nucleoside Diphosphate Kinase. *Biochemistry* **38:**4701–4711.

Balzarini J, Egberink H, Hartmann K, Cahard D, Vahlenkamp T, Thormar H, De Clercq E and Mcguigan C (1996) Antiretrovirus specificity and intracellular metabolism of 2′,3′-didehydro-2′,3′-dideoxythymidine (Stavudine) and its 5′-monophosphate triester prodrug So324. *Mol Pharmacol* **50:**1207–1213.

Balzarini J, Herdewijn P and De Clercq E (1989) Differential patterns of intracellular metabolism of 2′,3′-didehydro-2′,3′-dideoxythymidine (D4T) and 3′-azido-2′,3′-dideoxythymidine (AZT), two potent anti-HIV compounds. *J Biol Chem* **264:** 6127–6133.

Bourdais J, Biondi R, Lascu I, Sarfati S, Guerreiro C, Janin J and Véron M (1996) Cellular phosphorylation of anti-HIV nucleosides: Role of nucleoside diphosphate kinase. *J Biol Chem* **271:**7887–7890.

Bradford MM (1976) A rapid and sensitive method for the quantitation of microgram quantities of protein utilizing the principle of protein-dye binding. *Anal Biochem* **72:**248–254.

Cherfils J, Morera S, Lascu I, Véron M and Janin J (1994) X-ray structure of nucleoside diphosphate kinase complexed with dTDP and Mg^{++} at 2Å resolution. *Biochemistry* **33:**9062–9069.

Chiadmi M, Moréra S, Lascu I, Dumas C, LeBras G, Véron M and Janin J (1993) The Awd nucleoside diphosphate kinase from *Drosophila* structure. *Structure* **1:**283–293.

Deville-Bonne D, Sellam O, Merola F, Lascu I, Desmadril M and Véron M (1996) Phosphorylation of nucleoside diphosphate kinase at the active site studied by steady-state and time-resolved fluorescence. *Biochemistry* **35:**14643–14650.

Dumas C, Lascu I, Morera S, Glaser P, Fourme R, Wallet V, Lacombe M-L, Véron M and Janin J (1992) X-ray structure of nucleoside diphosphate kinase. *EMBO J* **11:**3203–3208.

Egron D, Lefebvre I, Périgaud C, Beltran T, Pompon A, Gosselin G, Aubertin A-M and Imbach J-L (1998) Anti-HIV pronucleotides: Decomposition pathways and correlation with biological activities. *Bioorg Med Chem Lett* **8:**1045–1050.

Foudraine NA, de Jong JJ, Weverling GJ, van Benthem BHB, Maas J, Keet IPM, Jurriaans S, Roos MTL, Vandermeulen K, de Wolf F and Lange JMA (1998) An open randomized controlled trial of zidovudine plus lamivudine versus stavudine plus lamivudine. *AIDS (Lond)* **12:**1513–1519.

Gao W, Agbaria R, Driscoll JS and Mitsuya H (1994) Divergent anti-human immunodeficiency virus activity and anabolic phosphorylation of 2′,3′-dideoxynucleoside analogs in resting and activated human cells. *J Biol Chem* **269:**12633–12638.

Garces E and Cleland WW (1969) Kinetic studies of yeast nucleoside diphosphate kinase. *Biochemistry* **8:**633–640.

Gill SC and Von Hippel PH (1989) Calculation of protein extinction coefficient from amino acid sequence data. *Anal Biochem* **182:**319–326.

Gonin P, Xu Y, Milon L, Dabernat S, Morr M, Kumar R, Lacombe M-L, Janin J and Lascu I (1999) Catalytic mechanism of nucleoside diphosphate kinase investigated using nucleotide analogs, viscosity effects and X-ray crystallography. *Biochemistry* **22:**7265–7272.

Hummel JP and Dreyer WJ (1962) Measurement of protein-binding phenomena by gel filtration. *Biochim Biophys Acta* **63:**530–532.

Kaul S, Dandekar KA, Schilling BE and Barbhaiya RH (1999) Toxicokinetics of 2′,3′-Didehydro-3′-deoxythymidine, Stavudine (D4T). *Drug Metab Dispos* **27:**1–12.

Krayevsky AA and Watanabe KA (1998) Substrates of DNA polymerases with planar conformation of sugar: Model of substrate transition state? *Nucleosides Nucleotides* **17:**1153–1162

Kunkel TA (1985) Rapid and efficient site-specific mutagenesis without phenotypic selection. *Proc Natl Acad Sci USA* **82:**488–492.

Lascu I, Chaffotte A, Limbourg-Bouchon B and Véron M (1992) A Pro/Ser substitution in nucleoside diphosphate kinase of *Drosophila melanogaster* (mutation killer of prune) affects stability but not catalytic efficiency of the enzyme. *J Biol Chem* **267:**12775–12781.

Lavie A, Vetter IR, Konrad M, Goody RS, Reinstein J and Schlichting I (1997) Structure of thymidylate kinase reveals the cause behind the limiting step in AZT activation. *Nat Struct Biol* **4:**601–604.

Milon L, Rousseau-Merck M, Munier A, Erent M, Lascu I, Capeau J and Lacombe M (1997) nm23–H4, a new member of the family of human nm23/nucleoside diphosphate kinase genes localised on chromosome 16p13. *Hum Genet* **99:**550–557.

Morera S, Lacombe M-L, Xu Y, LeBras G and Janin J (1995) X-ray structure of nm23 human nucleoside diphophate kinase B complexed with GDP at 2A resolution. *Structure* **3:**1307–1314.

Morera S, Lascu I, Dumas C, LeBras G, Briozzo P, Véron M and Janin J (1994) ADP binding and the active site of nucleoside diphosphate kinase. *Biochemistry* **33:** 459–467.

Munch-Petersen B, Cloos L, Tyrsted G and Eriksson S (1991) Diverging substrate specificity of pure human thymidine kinases 1 and 2 against antiviral dideoxynucleosides. *J Biol Chem* **266:**9032–9038.

Munier A, Feral C, Milon L, Phung-Ba Pinon V, Gyapay G, Capeau J, Guellaen G and Lacombe ML (1998) A new human *nm23* homologue (*nm23*-H5) specifically expressed in testis germinal cells. *FEBS Lett* **434:**289–294.

Ono K, Nagase H, Herdewjin P, Balzarini J and De Clercq E (1989) Differential inhibitory effects of several pyrimidine 2′,3′-dideoxynucleoside 5′-triphosphates on the activity of reverse transcriptases and various cellular DNA polymerases. *Mol Pharmacol* **35:**578–583.

Schaertl S, Konrad M and Geeves MA (1998) Substrate specificity of human nucleoside-diphosphate kinase revealed by transient kinetic analysis. *J Biol Chem* **273:**5662–5669.

Schneider B, Xu YW, Janin J, Véron M and Deville-Bonne D (1998a) 3′ phosphorylated nucleotides are tight binding inhibitors of nucleotide diphosphate kinase activity. *J Biol Chem* **273:**28773–28778.

Schneider B, Xu YW, Sellam O, Sarfati R, Janin J, Véron M and Deville-Bonne D (1998b) Pre-steady state of reaction of nucleoside diphosphate kinase with anti-HIV nucleotides. *J Biol Chem* **273:**11491–11497.

Tepper A, Dammann H, Bominaar AA and Véron M (1994) Investigation of the active site and conformational stability of nucleoside diphosphate kinase by site-directed mutagenesis. *J Biol Chem* **269:**32175–32180.

Venturelli D, Martinez R, Melotti P, Casella I, Peschle C, Cucco C, Spampinato G, Darzynkiewicz Z and Calabretta B (1995) Overexpression of DR-nm23, a protein encoded by a member of the nm23 gene family, inhibits granulocyte differentiation and induces apoptosis in 32Dc13 myeloid cells. *Proc Natl Acacd Sci USA* **92:**7435–7439.

Webb PA, Perisic O, Mendola CE, Backer JM and Williams RL (1995) The crystal structure of a human nucleoside diphosphate kinase, NM23–H2. *J Mol Biol* **251:**574–587.

Williams RL, Munoz-Dorado J, Jacobo-Molina A, Inouye S, Inouye M and Arnold E (1991) Crystallization and preliminary X-ray diffraction analysis of nucleoside diphosphate kinase from *Myxococcus xanthus*. *J Mol Biol* **220:**5–7.

Xu Y, Morera S, Janin J and Cherfils J (1997a) AlF3 mimics the transition state of protein phosphorylation in the crystal structure of nucleoside diphosphate kinase and MgADP. *Proc Natl Acad Sci USA* **94:**3579–3583.

Xu Y, Sellam O, Moréra S, Sarfati S, Biondi R, Véron M and Janin J (1997b) X-ray analysis of azido-thymidine diphosphate binding to nucleoside diphosphate kinase. *Proc Natl Acad Sci USA* **94:**7162–7165.

Zhu C, Johansson M, Permert J and Karlsson A (1998) Enhanced cytotoxicity of nucleoside analogs by overexpression of mitochondrial deoxyguanosine kinase in cancer cell lines. *J Biol Chem* **273:**14707–14711.

Send reprint requests to: Dominique Deville-Bonne, Unité de Régulation Enzymatique des Activités Cellulaires, Institut Pasteur, 25 rue du Dr. Roux, 75724 Paris Cedex 15, France. E-mail: ddeville@pasteur.fr